Astronomy & Astrophysics

LETTER TO THE EDITOR

Effect of rotational excitation of H₂ on isotopic exchange reaction with OD⁻ at low temperatures

Š. Roučka, S. Rednyk, A. Kovalenko, T. D. Tran, R. Plašil, Á. Kálosi, P. Dohnal, D. Gerlich, and J. Glosík

Department of Surface and Plasma Science, Faculty of Mathematics and Physics, Charles University, V Holešovičkách 2, 180 00 Prague, Czech Republic
e-mail: stepan.roucka@mff.cuni.cz

ABSTRACT

Aims. This paper presents experimentally obtained rate coefficients for the weakly endothermic reaction $OD^- + H_2 \rightarrow OH^- + HD$ with ortho- and para-hydrogen at astrophysically relevant temperatures between 10 and 300 K.
Methods. The reaction was studied with normal and para-enriched (99.5% para-H_2) hydrogen in a 22-pole ion trap. The measured temperature dependencies of reaction rate coefficients are analyzed using a model which assumes that the rotational energies of the two reactants are equivalent to the translational energy in driving the reaction.
Results. At room temperature, the rate coefficients of reactions with both nuclear spin variants reach 7×10^{-11} cm³ s⁻¹, which is in good agreement with the previous results from ion trap and swarm experiments with normal hydrogen. Cooling down the trap slows down the reaction and leads, at a nominal trap temperature of 11 K, to a rate coefficient below 10^{-14} cm³ s⁻¹ for para-enriched hydrogen. The fitted reaction endothermicity of 25.3 ± 2.2 meV agrees well with the literature value calculated in the Born-Oppenheimer approximation, $\Delta H^0 = 24.0$ meV. A simpler evaluation procedure, fitting the data with Arrhenius functions, results in ${}^p k = 16.8 \times 10^{-11} \exp(-234 \, \text{K}/T)$ cm³ s⁻¹ for pure para-hydrogen and ${}^o k = 9.4 \times 10^{-11} \exp(-101 \, \text{K}/T)$ cm³ s⁻¹ for pure ortho-hydrogen.

Key words. astrochemistry – molecular data – molecular processes – methods: laboratory: molecular – ISM: molecules

1. Introduction

In the present study we investigate the weakly endothermic H/D exchange reaction

$$OD^- + H_2 \xrightarrow{k_1} OH^- + HD, \qquad \Delta H^0 = 24.0 \text{ meV}. \tag{1}$$

Isotope exchange between different molecules is always nearly thermoneutral; however, due to differences in zero-point energies of the reactants and the products, endothermicities or exothermicities of some tens of meV are obtained. Hence, rate coefficients for H/D exchange tend to be very sensitive to temperatures between 10 and 1000 K, which are typical for the interstellar medium. One consequence is that deuterated molecular species are important tracers for the physical conditions prevailing in the interstellar medium (Roberts & Millar 2000). For example, observations of deuteration have been used, in combination with chemical models, to explore the origin of solar-system molecules (Cleeves et al. 2014b), to constrain the ionization rates in protoplanetary disks (Miettinen et al. 2011; Cleeves et al. 2014a), or to measure the age of prestellar cores (Pagani et al. 2013). The observations of the H/D ratios in molecules are generally concentrating on cations or neutrals, while not much is known about deuteration of anions. Negatively charged ions have recently been observed in space (McCarthy et al. 2006; Cernicharo et al. 2007; Brünken et al. 2007), and their role is increasingly more frequently investigated using astrochemical networks (Walsh et al. 2009; McElroy et al. 2013). In

particular, UMIST-based models (McElroy et al. 2013) predict that OH⁻ ions are present in cold dark clouds in quantities comparable to its positive counterpart, OH⁺. While OH and OH⁺ are routinely observed (see, e.g., Gerin et al. 2010; Wampfler et al. 2010), OH⁻ is still just a candidate for detection in space (Cazzoli & Puzzarini 2006).

The importance of the OH⁻ ion is underlined by a number of recent laboratory and theoretical studies of its destruction (Hlavenka et al. 2009; Hauser et al. 2015a), formation (Jusko et al. 2015; Plašil et al. 2017), inelastic collisions (Hauser et al. 2015b), or its rotational spectrum (Cazzoli & Puzzarini 2006; Matsushima et al. 2006; Jusko et al. 2014; Lee et al. 2016). Additionally, the OH⁻ anion has become a tool for thermometry of ions in ion traps (Otto et al. 2013; Endres et al. 2017) and storage rings (DESIREE, Schmidt et al. 2017; CSR, Meyer et al. 2017), based on threshold photodetachment spectroscopy.

This work presents rate coefficients measured for reaction (1) with normal and para-enriched H₂ at trap temperatures ranging from 10 to 300 K. Previous studies, performed at room temperature (Grabowski et al. 1983) or in the ranges of 10–300 K (Mulin et al. 2015) and 300–508 K (Viggiano & Morris 1994), used only normal H₂. Experimental determination of state-specific rate coefficients for $J_{H_2} = 0$ and 1 is essential because the reactivity is highly sensitive to the internal excitation of the reactants. Moreover, the interstellar ortho-/para-H₂ population is often far from thermal equilibrium.
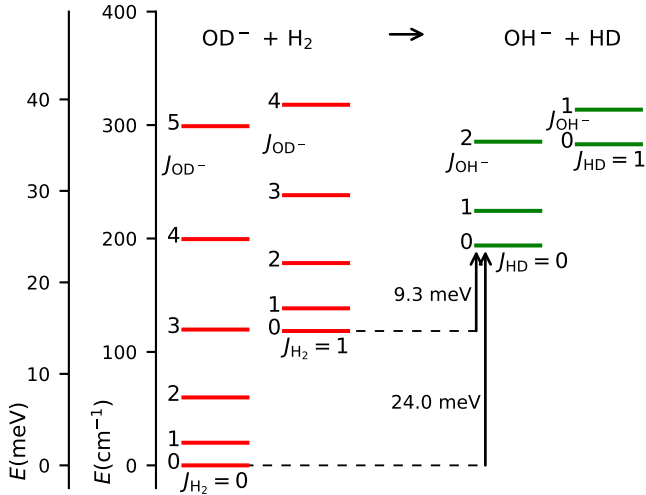
Fig. 1. Rotational energy levels of the reactants (left-hand side) and products (right-hand side) for reaction (1). The rotational constants for OD^-, OH^-, HD, and H_2 are taken from the literature (Huber & Herzberg 1979; Rehfuss et al. 1986; Matsushima et al. 2006). The two arrows indicate that 24.0 meV of translational energy are needed to reach the threshold at 0, while 9.3 meV are sufficient for reaction with ortho-H_2 ($J_{H_2} = 1$).

To compare internal excitation with the endothermicity, Fig. 1 shows the lowest rotational states of the involved diatomic molecules. The nuclear spin states $I = 0$ (para) and 1 (ortho) are linked to the even and odd rotational states, respectively. The 0 K reaction enthalpy of 24 meV was calculated in the Born-Oppenheimer approximation, as discussed in detail by Mulin et al. (2015). At meV accuracy, the energetics are influenced by isotopic electronic shifts of the potential energy surfaces of OD^- and OH^-, as shown for several other isotope exchange reactions with H_2 and D_2 (Kleinman & Wolfsberg 1973, 1974; Adohi-Krou et al. 2004). In particular, spectroscopic studies of OH and OD neutrals suggest that the isotopic shift of electronic ground-state potential energy surface in this system can be up to 2.5 meV (see note 78 in Ruscic et al. 2002). We here also derive an experimental value of the reaction endothermicity.

2. Experiment

The experiments have been carried out using the RF 22-pole ion trap machine described by Gerlich (1995, 2008) and Zymak et al. (2011). This instrument has been used to study isotope effects in anion–neutral reactions (Mulin et al. 2015; Roučka et al. 2015; Plašil et al. 2017), therefore we only recall a few specific details. The 22-pole trap was operated at an RF frequency of 17.4 MHz and at amplitudes up to 60 V. The nominal trap temperature (T_{22PT}) was varied from 300 K down to 10 K.

OD^- ions were produced in an electron impact storage ion source (SIS) using a mixture of N_2O and D_2 (Jusko et al. 2013, 2014). They were extracted from the source, mass selected by a quadrupole mass filter, and guided into the ion trap, where reactions with H_2 were followed as a function of time and H_2 number density. A He/H_2 gas mixture was introduced directly into the trap volume. After various well-defined trapping times, the trap was opened and ions were extracted, mass selected by a second quadrupole mass spectrometer, and counted by an MCP detector. The numbers of detected ions were proportional to the numbers of trapped ions, and minor differences in the overall

detection efficiency for OD^- and OH^- were accounted for in the data analysis.

The addition of helium buffer gas ensures that most of the ions are collisionally thermalized before reacting with H_2. Typically used He/H_2 mixtures result in ten collisions with He for every one collision with H_2 on average. Moreover, at low temperatures, H_2 molecules also act as a buffer gas because of the low probability for a reactive collision. Recent experiments in our apparatus (Plašil et al. 2012; Zymak et al. 2013) as well as in other 22-pole trap experiments (Hauser et al. 2015b; Endres et al. 2017) have confirmed that the collisional temperature is slightly higher than the temperature of the trap. In the present case we can safely assume that the collisional temperature in interaction of OD^- with H_2 does not exceed the trap temperature by more than 10 K. For simplicity of presentation, we define the collisional temperature as $T = T_{22PT} + 5$ K with an uncertainty of ±5 K.

We used normal hydrogen ($^n H_2$) and para-enriched hydrogen ($^e H_2$) as reactants, with number densities varying from 10^{12} up to 10^{13} cm^{-3}. In normal H_2, the para/ortho ratio is 1/3, corresponding to the 300 thermal equilibrium. The para-enriched hydrogen, containing 99.5% of para-H_2, was produced using a para-hydrogen generator with paramagnetic catalyst (Hejduk et al. 2012; Dohnal et al. 2012; Zymak et al. 2013). The amount of ortho impurities was determined in situ using chemical probing with N^+ ions (Zymak et al. 2013). The nuclear spin-state-specific rate coefficients $^p k_1$ and $^o k_1$ for the reaction of OD^- with para- and ortho-H_2 were then calculated from the measured rate coefficients $^n k_1$ and $^e k_1$ for the reaction with $^n H_2$ and with $^e H_2$.

To evaluate the measured time dependencies, especially at low temperatures, we have to take into account reconversion of OH^- products back to OD^- via the fast exothermic reaction (Mulin et al. 2015)

$$OH^- + D_2 \xrightarrow{k_2} OD^- + HD, \qquad \Delta H^0 = -17.2 \text{ meV}. \tag{2}$$

The D_2 traces in the trap originate from the ion source. Equilibrium between this backward reconversion reaction and reaction (1) is established at long enough trapping times.

3. Results and discussion

The change in numbers of detected OD^- and OH^- ions in the trap can be described with the balance equations

$$\frac{d N_{OD^-}}{d t} = -k_1 N_{OD^-}[H_2] + k_2 \xi N_{OH^-}[D_2], \tag{3}$$

$$\frac{d N_{OH^-}}{d t} = -k_2 N_{OH^-}[D_2] + k_1 \frac{N_{OD^-}}{\xi}[H_2], \tag{4}$$

where k_1 and k_2 are the rate coefficients of reactions (1) and (2), and [H_2] and [D_2] are the number densities of H_2 and D_2 in the trap, respectively. The factor ξ, which is close to 1, accounts for the detection efficiency of OD^- relative to OH^-. In the following, the additional index n and e is used, that is, $^n k_i$ and $^e k_i$, to indicate reactions with $^n H_2$ and $^e H_2$, respectively. The reaction rate coefficients are determined by fitting the measured time dependencies of the numbers of detected ions, $N_{OD^-}(t)$ and $N_{OH^-}(t)$, with solution of Eqs. (3) and (4). Free parameters of the fit are the reaction rates $r_1 = k_1[H_2]$ and $r_2 = k_2[D_2]$, the initial numbers of detected ions, $N_{OD^-}(t = 0)$ and $N_{OH^-}(t = 0)$, and the relative detection efficiency ξ.
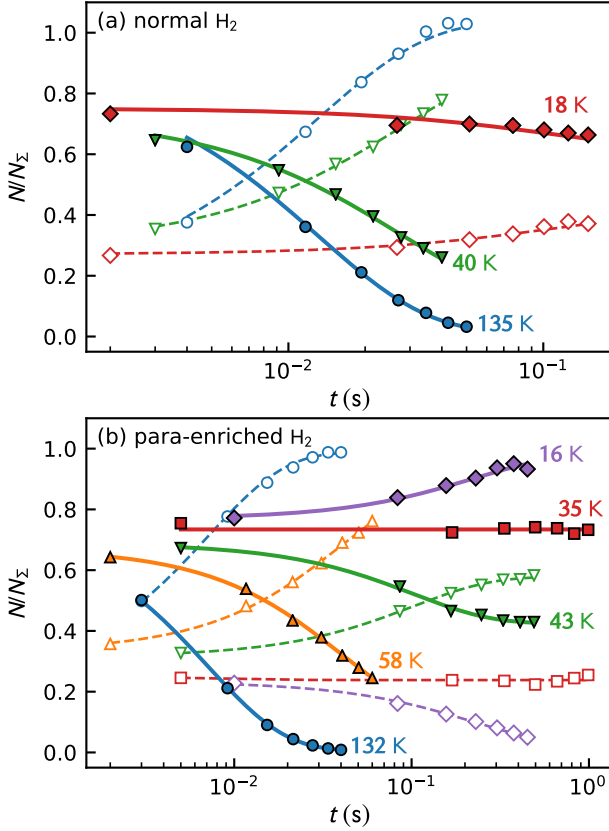
Fig. 2. Time dependencies of the normalized numbers of OD^- (filled symbols) and OH^- (open symbols), measured with $^nH_2$ (*panel a*) and $^eH_2$ (*panel b*). The collisional temperatures are indicated in the figure, and the densities of $^nH_2$, $^eH_2$, He, and D_2 are listed in Table 1.

Table 1. Experimental conditions (collisional temperatures T, number densities of H_2, He, and D_2, and fractions of ortho-H_2) used to measure the data shown in Fig. 2.

$\dfrac{T}{K}$	$\dfrac{[H_2]}{10^{12}\ cm^{-3}}$	$\dfrac{[^oH_2]}{[H_2]}$	$\dfrac{[He]}{10^{12}\ cm^{-3}}$	$\dfrac{[D_2]}{10^9\ cm^{-3}}$
135	1.8	0.75	16	3.0
40	6.8	0.75	30	5.4
18	10.3	0.75	45	8.2
132	3.7	0.005	22	2.2
58	7.2	0.005	33	3.3
43	8.3	0.005	38	3.8
35	9.2	0.005	42	4.2
16	10.4	0.005	33	6.3

Notes. The H_2 and He gases are introduced to the trap volume via the inlet system, and D_2 is diffusing into the trap from the ion source. The uncertainties of the number densities are close to 20%.
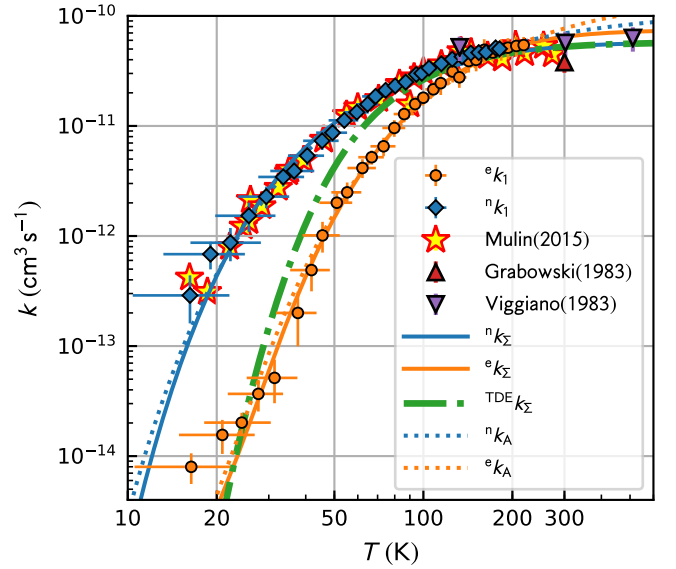

Fig. 3. Temperature dependencies of the rate coefficients, $^nk_1$ and $^ek_1$, measured for reaction (1) with $^nH_2$ and with $^eH_2$. We also plot data obtained in our previous experiments with $^nH_2$ using the same experimental arrangement (Mulin et al. 2015), FDT data of Viggiano & Morris (1994), and SIFT data of Grabowski et al. (1983). The solid and dotted lines show the result of a state-specific model and an Arrhenius model, respectively. For details, see the text. The dash-dotted line indicates the thermal rate coefficient, i.e., the ortho/para ratio is also equilibrated to T.

Examples of measured and fitted time dependencies are plotted in Fig. 2. For clarity, the numbers are normalized by the total number of ions, N_Σ, measured directly after filling the trap. The upper panel of Fig. 2 shows data obtained with $^nH_2$ as target gas, and the lower panel those for $^eH_2$. The corresponding densities of $^nH_2$, $^eH_2$, He, and D_2 in the trap are listed in Table 1. The density of D_2 penetrating from the ion source is typically 1000 times lower than that of H_2. Nevertheless, the equilibrium numbers of OD^- are comparable to or even higher than those of OH^- at the lowest temperatures because of the very slow forward reaction and the fast backward reconversion reaction. The effect of backward reconversion is even more pronounced for a reaction with para-enriched H_2. The dependence of the reaction rate r_1 on the hydrogen number density was measured to be linear, confirming the binary character of reaction (1).

Figure 3 compares the rate coefficients, $^nk_1$ and $^ek_1$, measured between 15 and 300 with previous results for $^nk_1$ from the same experimental arrangement (Mulin et al. 2015; shown as a function of collisional temperature, $T = T_{22PT} + 5$ K). The agreement is very good (within a few percent). We also show results from the FDT experiment of Viggiano & Morris (1994) and the SIFT experiment of Grabowski et al. (1983). The data we present were simplified by binning the results of nearly 300 measurements into logarithmically spaced bins in temperature. The indicated uncertainties of the reaction rate coefficients take into account the estimated fit errors and the 5 uncertainty of the collisional temperature, which also influences the reactant number density. The uncertainty due to pressure measurement is 20%.

The Arrhenius plot of the measured reaction rate coefficients shown in Fig. 4 reveals a nearly linear dependence of $^nk_1$ and $^ek_1$ over two and three orders of magnitude, respectively. The deviations from linearity for temperatures below 25 are smaller than the estimated temperature uncertainty of ±5 K.

We analyzed our data using the simple statistical model described by Mulin et al. (2015), which takes into account any non-equilibrium population of H_2 rotational states. Generally, the rate coefficient k_1 of reaction (1) can be expressed as a weighted sum k_Σ of state-specific rate coefficients $k_{J_{H_2}\,J_{OD^-}}$, averaged over the rotational states J_{H_2} and J_{OD^-} of H_2 and OD^-. In particular, we define rate coefficients $^nk_\Sigma$ and $^ek_\Sigma$ for reaction with normal and para-enriched H_2 as

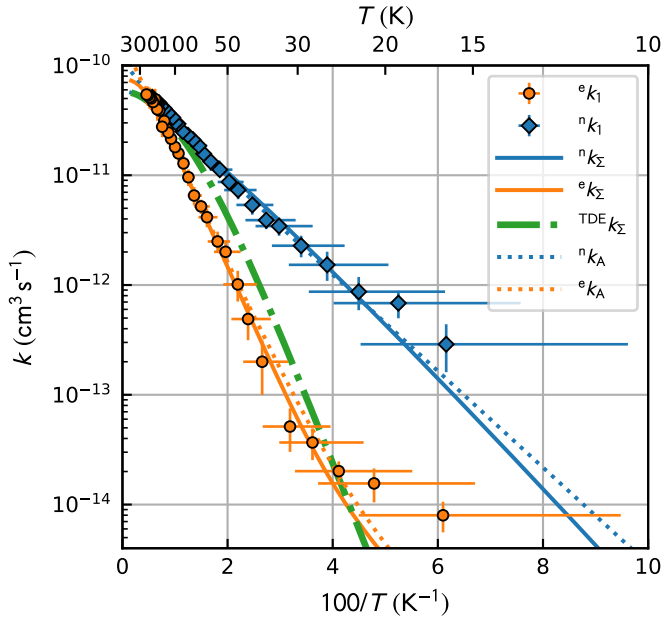$$^{n/e}k_\Sigma = \sum_{J_{H_2},J_{OD^-}} {}^{n/e}P_{J_{H_2}} P_{J_{OD^-}} k_{J_{H_2}\,J_{OD^-}}, \qquad (5)$$

Fig. 4. Arrhenius plot of $^{e}k_1$ and $^{n}k_1$ measured in experiments with $^{e}H_2$ and $^{n}H_2$. The solid and dotted lines show the results from a state-specific model and an Arrhenius model, respectively. The dash-dotted line shows the fully thermalized rate coefficients. For details, see the text.

where $^{n/e}P_{J_{H_2}}$ and $P_{J_{OD^-}}$ are the corresponding populations of rotational states. Our model uses the assumption that all state-specific rate coefficients follow the Arrhenius temperature dependence

$$k_{J_{H_2} J_{OD^-}} = {}^{p/o}k_0 \exp\left(-\frac{\Delta E_{J_{H_2} J_{OD^-}}}{k_B T}\right), \qquad (6)$$

with the activation energy given by

$$\Delta E_{J_{H_2} J_{OD^-}} = \max\left\{0, \Delta H_{fit}^0 - E_{J_{H_2}} - E_{J_{OD^-}}\right\}. \qquad (7)$$

The model assumes that both the rotational energy of $E_{J_{H_2}}$ and $E_{J_{OD^-}}$ and the translational energy are equivalent in driving the reaction. In Eq. (6) we also assume that there is a global pre-exponential factor $^{p}k_0$ for reactions with para-H_2 (J_{H_2} even) and $^{o}k_0$ for all reactions of ortho-H_2 (J_{H_2} odd). The only free parameters of the model are the reaction endoergicity ΔH_{fit}^0 and the pre-exponential factors $^{p}k_0$ and $^{o}k_0$. The model was fitted globally to both temperature dependencies of rate coefficients of reactions with ortho- and para-H_2, resulting in

$$\Delta H_{fit}^0 = 25.3_{-2.1}^{+2.4}\,\text{meV},$$
$$^{p}k_0 = 7.4_{-0.4}^{+0.7} \times 10^{-11}\,\text{cm}^3\,\text{s}^{-1}, \quad ^{o}k_0 = 5.2_{-1.3}^{+1.3} \times 10^{-11}\,\text{cm}^3\,\text{s}^{-1}.$$

These mean values were obtained from fits corresponding to the collisional temperature $T = T_{22PT} + 5\,\text{K}$. The quoted uncertainties include the statistical errors and the systematic errors due to temperature uncertainty, which were estimated by fitting the data with collisional temperatures defined as $T^- = T_{22PT}$ and $T^+ = T_{22PT} + 10\,\text{K}$. The pre-exponential factors $^{p}k_0$ and $^{o}k_0$ have additional uncertainty of 20% due to the uncertainty of the pressure. The fitted curves are included in Figs. 3 and 4.

The true thermal reaction rate coefficient $^{TDE}k_\Sigma$ plotted in Figs. 3 and 4 was derived from our model by inserting the equilibrium population of all H_2 rotational states, $^{TDE}P_{J_{H_2}}$, into Eq. (5), that is, also assuming equilibrium ortho/para population.

To facilitate the incorporation of our data into chemical models, we also fit our data with the simple Arrhenius model, described by the equation

$$^{n/e}k_A = (1 - {}^{n/e}f)\,{}^{p}k_A + {}^{n/e}f\,{}^{o}k_A, \qquad (8)$$

where $^{n/e}f = [^{o}H_2]/[^{n/e}H_2]$ is the fraction of ortho-H_2 in the normal/para-enriched H_2 and

$$^{p/o}k_A = {}^{p/o}k_{A0} \exp(-{}^{p/o}E_A/(k_B T)). \qquad (9)$$

The agreement of the fit with our data (Fig. 4) indicates that the linear combination of Arrhenius dependencies (8) is a good approximation. The resulting parameters are

$$^{o}E_A = 8.7_{-1.7}^{+2.1}\,\text{meV}, \qquad ^{o}k_{A0} = 9.4_{-2.2}^{+3.1} \times 10^{-11}\,\text{cm}^3\,\text{s}^{-1},$$
$$^{p}E_A = 20.1_{-2.3}^{+2.7}\,\text{meV}, \qquad ^{p}k_{A0} = 16.8_{-2.7}^{+3.6} \times 10^{-11}\,\text{cm}^3\,\text{s}^{-1}.$$

The errors were estimated by the same procedure as discussed above for the state-specific model parameters.

The fitted endothermicity ΔH_{fit}^0 is in good agreement with the value $\Delta H^0 = 24.0\,\text{meV}$ discussed in the Introduction. This confirms that the isotopic energy shifts are not significantly larger than our experimental accuracy ($\approx 2.5\,\text{meV}$). The discrepancy between the Arrhenius activation energy $^{p}E_A$ and the endothermicities ΔH_{fit}^0 and ΔH^0 is not surprising because $^{p}E_A$ is an empirical parameter that does not account for the internal excitation of the reactants. Nevertheless, the activation energy $^{o}E_A$ of the reaction with ortho-H_2 is in good agreement with the Born-Oppenheimer estimate of 9.3 meV. It is also in agreement with the activation energy of reaction with normal H_2, $E_{A\text{-}exp} = (7.9 \pm 0.3)\,\text{meV}$ determined by Mulin et al. (2015), which confirms that reaction with ortho-H_2 was the dominant process in that experiment.

4. Conclusions

We have extended our previous measurements (Mulin et al. 2015) of the isotope exchange reaction between OD$^-$ and H_2 using nearly pure para-hydrogen. The data allowed us to extract nuclear-spin specific rate coefficients at temperatures from 15 to 300 . As expected, the two results are equal at room temperature and agree well with previous data (Viggiano & Morris 1994; Grabowski et al. 1983). Over a wide range of temperatures, the rate coefficients fall with decreasing temperature in accordance with the Arrhenius formula. For astrochemical models, reactions with pure para- or ortho-H_2 can be simply characterized with Arrhenius functions $^{p}k = 16.8 \times 10^{-11} \exp(-234\,\text{K}/T)\,\text{cm}^3\,\text{s}^{-1}$ and $^{o}k = 9.4 \times 10^{-11} \exp(-101\,\text{K}/T)\,\text{cm}^3\,\text{s}^{-1}$, respectively.

References

Adohi-Krou, A., Martin, F., Ross, A. J., Linton, C., & Le Roy R. J. 2004, J. Chem. Phys., 121, 6309
Brünken, S., Gupta, H., Gottlieb, C. A., McCarthy, M. C., & Thaddeus, P. 2007, ApJ, 664, L43
Cazzoli, G., & Puzzarini, C. 2006, ApJ, 648, L79
Cernicharo, J., Guélin, M., Agúndez, M., et al. 2007, A&A, 467, L37
Cleeves, L. I., Bergin, E. A., & Adams, F. C. 2014a, ApJ, 794, 123
Cleeves, L. I., Bergin, E. A., Alexander, C. M. O., et al. 2014b, Science, 345, 1590

Dohnal, P., Hejduk, M., Varju, J., et al. 2012, Phil. Trans. R. Soc. A, 370, 5101

Endres, E. S., Egger, G., Lee, S., et al. 2017, J. Mol. Spectr., 332, 134

Gerin, M., De Luca, M., Black, J., et al. 2010, A&A, 518, L110

Gerlich, D. 1995, Phys. Scr., 1995, 256

Gerlich, D. 2008, Low Temperatures and Cold Molecules (London: Imperial College Press)

Grabowski, J. J., DePuy, C. H., & Bierbaum, V. M. 1983, J. Am. Chem. Soc., 105, 2565

Hauser, D., Lakhmanskaya, O., Lee, S., Roučka, Š., & Wester, R. 2015a, New J. Phys.

Hauser, D., Lee, S., Carelli, F., et al. 2015b, Nat. Phys., 11, 467

Hejduk, M., Dohnal, P., Varju, J., et al. 2012, Plasma Sources Sci. Technol., 21, 024002

Hlavenka, P., Otto, R., Trippel, S., et al. 2009, J. Chem. Phys., 130, 061105

Huber, K. P., & Herzberg, G. 1979, Molecular Spectra and Molecular Structure: Constants of Diatomic Molecules (New York: Van Nostrand Reinhold)

Jusko, P., Roučka, Š., Plašil, R., & Glosík, J. 2013, Int. J. Mass Spectrom., 352, 19

Jusko, P., Asvany, O., Wallerstein, A.-C., Brünken, S., & Schlemmer, S. 2014, Phys. Rev. Lett., 112, 253005

Jusko, P., Roučka, Š., Mulin, D., et al. 2015, J. Chem. Phys., 142, 014304

Kleinman, L. I., & Wolfsberg, M. 1973, J. Chem. Phys., 59, 2043

Kleinman, L. I., & Wolfsberg, M. 1974, J. Chem. Phys., 60, 4740

Lee, S., Hauser, D., Lakhmanskaya, O., et al. 2016, Phys. Rev. A, 93, 032513

Matsushima, F., Yonezu, T., Okabe, T., Tomaru, K., & Moriwaki, Y. 2006, J. Mol. Spectrosc., 235, 261

McCarthy, M. C., Gottlieb, C. A., Gupta, H., & Thaddeus, P. 2006, ApJ, 652, L141

McElroy, D., Walsh, C., Markwick, A. J., et al. 2013, A&A, 550, A36

Meyer, C., Becker, A., Blaum, K., et al. 2017, Phys. Rev. Lett., 119, 023202

Miettinen, O., Hennemann, M., & Linz, H. 2011, A&A, 534, A134

Mulin, D., Roučka, Š., Jusko, P., et al. 2015, Phys. Chem. Chem. Phys., 17, 8732

Otto, R., von Zastrow, A., Best, T., & Wester, R. 2013, Phys. Chem. Chem. Phys., 15, 612

Pagani, L., Lesaffre, P., Jorfi, M., et al. 2013, A&A, 551, A38

Plašil, R., Zymak, I., Jusko, P., et al. 2012, Phil. Trans. R. Soc. A, 370, 5066

Plašil, R., Tran, T. D., Roučka, Š., et al. 2017, Phys. Rev. A, 96, 062703

Rehfuss, B. D., Crofton, M. W., & Oka, T. 1986, J. Phys. Phys., 85, 1785

Roberts, H., & Millar, T. J. 2000, A&A, 361, 388

Roučka, Š., Mulin, D., Jusko, P., et al. 2015, J. Phys. Chem. Lett., 6, 4762

Ruscic, B., Wagner, A. F., Harding, L. B., et al. 2002, J. Phys. Chem. A, 106, 2727

Schmidt, H. T., Eklund, G., Chartkunchand, K. C., et al. 2017, Phys. Rev. Lett., 119, 073001

Viggiano, A. A., & Morris, R. A. 1994, J. Chem. Phys., 100, 2748

Walsh, C., Harada, N., Herbst, E., & Millar, T. J. 2009, ApJ, 700, 752

Wampfler, S. F., Herczeg, G. J., Bruderer, S., et al. 2010, A&A, 521, L36

Zymak, I., Jusko, P., Roučka, Š., et al. 2011, Eur. Phys. J. Appl. Phys., 56, 24010

Zymak, I., Hejduk, M., Mulin, D., et al. 2013, ApJ, 768, 86